Thermal-neutron capture by magnesium isotopes

T. A. Walkiewicz* and S. Raman
Oak Ridge National Laboratory, Oak Ridge, Tennessee 37831

E. T. Jurney, J. W. Starner, and J. E. Lynn
Los Alamos National Laboratory, Los Alamos, New Mexico 87545
(Received 26 August 1991)

We have studied the primary and secondary γ rays (33 in ^{25}Mg, 212 in ^{26}Mg, and 35 in ^{27}Mg) following thermal-neutron capture by the stable ^{24}Mg, ^{25}Mg, and ^{26}Mg isotopes. Almost all of these γ rays have been incorporated into the corresponding level schemes consisting of 9 excited levels in ^{25}Mg, 55 in ^{26}Mg, and 10 in ^{27}Mg. In each case, the observed γ rays account for nearly 100% of all captures. The measured neutron separation energies for ^{25}Mg, ^{26}Mg, and ^{27}Mg are, respectively, 7330.65±0.05, 11 093.18±0.05, and 6443.40±0.05 keV. The measured thermal-neutron capture cross sections for ^{24}Mg, ^{25}Mg, and ^{26}Mg are, respectively, 54.1±1.3, 200±3, and 39.0±0.8 mb. In all three cases, primary electric-dipole ($E1$) transitions account for the bulk of the total capture cross section. We have calculated these $E1$ partial cross sections using direct-capture theory. We have also speculated on the mechanism responsible for the magnetic-dipole ($M1$) transitions which are quite strong in ^{26}Mg.

PACS number(s): 25.40.Lw, 27.30.+t

I. INTRODUCTION

In a series of recent papers [1–6] on slow-neutron capture by light nuclides (^{7}Li, ^{9}Be, ^{12,13}C, ^{32,33,34}S, and ^{40,42,44,46,48}Ca), we have assessed, in a quantitative manner, the importance of the direct-capture mechanism within an optical-model framework. In these cases, we have demonstrated that direct capture, as originally formulated by Lane and Lynn [7] and further developed in Refs. [1–3], is indeed the predominant mechanism, and the remaining (usually small) discrepancies between experiment and theory can be plausibly attributed to contributions from the more complicated and statistically oriented compound-nuclear contributions from local unbound levels. The direct-capture mechanism is quite simple—a neutron that is initially in an s orbit in the overall potential field of the target nucleus falls into a p-wave orbit in the final nucleus resulting in the emission of an electric-dipole ($E1$) primary transition. The theoretical analysis *requires* knowledge of the coherent scattering length, the energies of these primary transitions, and the (d,p) spectroscopic strengths for the corresponding final states.

In this paper we study the primary and secondary γ rays following thermal-neutron capture by the stable ^{24}Mg, ^{25}Mg, and ^{26}Mg isotopes. In all three cases, $E1$ primary transitions account for the bulk of the total capture cross section. We calculate these $E1$ partial cross sections using direct-capture theory employing the same methods as developed in the earlier papers. In particular, we use the two methods of calculating the direct-capture cross section, namely, by use of (a) a "specialized" optical-model (S) (optical-model parameters specialized to the particular nuclide in question) and (b) a combination of global optical model plus a valence contribution ($G+V$) from levels near the neutron separation energy. The arguments for the use of these methods are summarized in Refs. [2] and [3] and are not repeated here. We find that direct capture accounts for the cross sections of primary $E1$ transitions in the three isotopes to within a factor of 2 (see Sec. IV). This is not such good agreement compared to many other nuclides that have been studied, but the differences can still be accounted for by invoking a relatively small admixture of truly compound-nuclear capture due to nearby levels.

Although the bulk of the capture is accounted for by $E1$ transitions, the $M1$ contribution is not negligible, especially in capture by ^{25}Mg. There is some indication that the strong $M1$ transitions are associated with final states having significant single-particle $l_n=0$ character. We have therefore compared these strengths with a magnetic-dipole version of the direct-capture theory [6]. This analysis, with its conclusion that direct capture fails to provide an adequate explanation of the strength of these $M1$ transitions, is described in Sec. V.

II. MEASUREMENTS

The (n,γ) measurements were carried out with enriched magnesium targets (see Table I) obtained from the Research Materials Collection maintained by the Oak Ridge National Laboratory. Measurements were also made with natural magnesium metal and oxide targets. Each target was studied in the thermal column of the internal target facility at the Los Alamos Omega West Reactor. This facility and the data analysis procedures have been described in detail in Ref. [1]. Gamma-ray

*Permanent address: Edinboro University of Pennsylvania, Edinboro, PA 16444.

TABLE I. Compositions of targets employed in this work.

Constituent	Thermal (n,γ) cross section	^{24}MgO 1.997 g	^{25}MgO 1.987 g	^{26}MgO 1.911 g
	(a) Isotopic enrichment (%)			
^{24}Mg	54 mb	99.94	1.86	0.21
^{25}Mg	200 mb	0.04	97.87	0.09
^{26}Mg	39 mb	0.02	0.26	99.70
	(b) Impurity concentration (approximate value in ppm)			
Gd	49000 b	0.7	0.3	0.2
Sm	5800 b	0.2	0.03	0.5
Cd	2450 b	1	40	5
Cl	33 b	50	230	27
Sc	26 b	24	65	35
Ti	6 b	20	30	17
S	520 mb	2900	290	300
Ca	430 mb	430	150	200
Si	160 mb	1300	900	1100

spectra were obtained with a 30-cm^3 coaxial intrinsic Ge detector positioned inside a 20-cm-diam by 30-cm-long NaI(Tl) annulus. Figure 1 shows the type of spectra (those with an enriched ^{25}Mg target) obtained in our measurements. The Ge detector was operated either in the Compton-suppressed mode (0.362 keV/channel) or in the pair-spectrometer mode (1.223 keV/channel). The latter mode utilizes the lengthwise optical division of the annulus so that only double-escape peaks appear in the pulse-height spectrum. At lower energies the two annulus halves are connected together electrically to operate in the conventional anticoincidence mode. In this mode, the full width at half maximum (FWHM) values for our system were 1.5, 1.8, 2.3, and 2.9 keV, respectively, for γ-ray energies of 0.5, 1.0, 2.0, and 3.0 MeV. In the pair-spectrometer mode, the FWHM values were 2.5, 3.3, 4.0, and 4.7 keV, respectively, for γ-ray energies of 3, 5, 7, and 9 MeV.

Energy calibrations in the double-escape mode were performed with the prompt γ-ray spectrum from neutron capture in melamine ($C_3H_6N_6$). In the anticoincidence mode, the prompt γ ray from the ^{1}H(n,γ) reaction plus the annihilation radiation were employed for this purpose. In both modes, nonlinearity corrections to the measured energies were made, using precisely known γ rays appropriate to the range of energies of interest. The primary calibration energies were those recommended most recently by Wapstra [8]: 511.000±0.002 keV for the annihilation radiation, 2223.253±0.004 keV for the γ ray from the ^{1}H(n,γ) reaction, and 4945.303±0.030 keV for the ground-state transition in the ^{12}C(n,γ) reaction. Secondary calibration energies were provided by several two-step cascades in the ^{14}N(n,γ) reaction.

Intensity calibrations were determined in the Compton-suppressed mode with a set of standard radioisotopic sources with precalibrated γ-ray intensities and were further checked with γ rays from ^{82}Br decay produced *in situ* in the internal target position. The efficiency curve in the pair-spectrometer mode was derived from the relative intensities of γ rays from the ^{14}N(n,γ) reaction as discussed in Ref. [9]. All capture cross sections reported here are based on σ_γ(2200 m/s)=332.6±0.7 mb for ^{1}H (Ref. [10]). The effect of possible variations in neutron flux was taken into account by normalizing the data to the neutron fluence for each run measured with a small fission counter located near the target position in the thermal column.

The ^{24}Mg(n,γ) reaction has been studied previously at Petten by Spilling, Gruppelaar, and op den Kamp [11]; at Grenoble by Hungerford and Schmidt [12]; and at McMaster by Prestwich and Kennett [13] with natural magnesium (79.0% ^{24}Mg) targets (oxide in the Grenoble case and metal in the other two). (The McMaster study [13] was limited to $E_\gamma > 1.4$ MeV in just the pair-spectrometer mode.) These three studies also provided some information on the ^{25}Mg(n,γ) and ^{26}Mg(n,γ) reactions due to the presence of 10.0% ^{25}Mg and 11.0% ^{26}Mg in natural magnesium. (With a natural target, captures in the ^{24}Mg, ^{25}Mg, and ^{26}Mg isotopes are 62%, 32%, and 6%, respectively.) Measurements with an 85% enriched

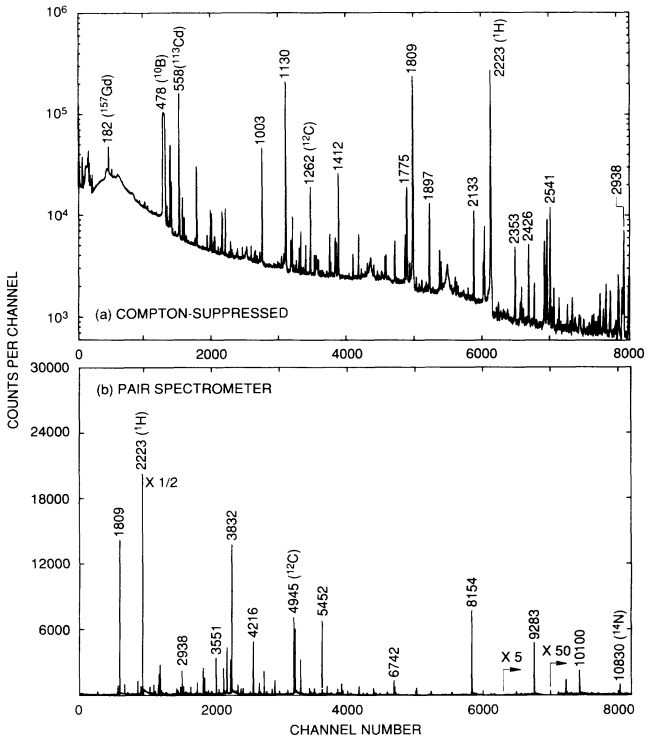

FIG. 1. Gamma-ray spectra from thermal neutron capture by ^{25}Mg. All energies are in keV. A detailed list of γ rays observed in ^{26}Mg is given in Table II(C).

^{25}Mg were also made in the course of the Petten studies [11]. Subsequently, Selin in collaboration with Hardell [14] and with Wallander [15], respectively, carried out (n,γ) studies at the Stockholm reactor with enriched (99.2%) ^{25}Mg and (98.7%) ^{26}Mg targets. The results of all of these studies have been evaluated by Endt [16] in arriving at his adopted level schemes for ^{25}Mg, ^{26}Mg, and ^{27}Mg.

While our primary aim in this experiment was to reliably measure the absolute partial cross sections of the primary $E1$ transitions in ^{25}Mg, ^{26}Mg, and ^{27}Mg for later comparisons with theory, the current spectroscopic data, especially for capture by ^{25}Mg and ^{26}Mg, are more extensive and definitive than previous (n,γ) studies for these nuclides. Even so, the enriched targets that we used were not pure enough to fully exploit all our capabilities. Numerous γ rays were present in the spectra, notably those due to gadolinium, chlorine, and cadmium, and interfered with the measurements. A detailed study was undertaken to identify the responsible contaminants. The resulting impurity concentrations for each target are presented in Table I. These results are consistent with the spectrographic analyses provided with the targets. Attempts to reduce the level of contaminants through chemical procedures were only partially successful; however, spectra under similar conditions were obtained from the natural elements listed in Table I and from several other commonly occurring elements to aid in the identification of peaks due to impurities and to correct for them in case of interference.

III. RESULTS

A. Reaction ^{24}Mg$(n,\gamma)^{25}$Mg

The energies and intensities of 33 γ rays assigned to ^{25}Mg are given in Table II(A) in addition to three γ rays for which upper intensity limits were obtained. The level scheme resulting from this work is presented in Table III(A). All γ rays but one (at 3660 keV) have been incorporated into this scheme consisting of nine excited states. The level energies listed in Table III(A) [the same applies for III(B) and III(C) also] were obtained through an overall least-squares fit involving all transitions. In deducing them, nuclear recoil was taken into account. The intensity balance for each of the nine excited states is good [see Table IV(A)]. The branching ratios for each excited state observed in this work are also in good agreement with the corresponding values given by Endt [16].

The J^{π} assignments listed in Table IV(A) [the same applies for IV(B) and IV(C) also] are from the latest compilation [16]. The two $E1$ primary transitions [see deexciting γ rays from the capturing state in Table III(A)] of energies 3917 and 3054 keV in ^{25}Mg account for 95% of the observed intensity of 54.3 mb out of the capturing state. The weakest transition observed was an $E2$ primary transition to the ground state with a cross section of only 18 μb, but, as a general rule, we have ignored transitions that are weaker than ~ 50 μb (~ 1 photon per 1000 neutron captures) unless their inclusion was warranted for branching-ratio purposes.

We found no evidence for any significant population of the 1612-keV, $\frac{7}{2}^+$ level [16]. The $\sim$1614-keV γ ray, shown as deexciting this state in Ref. [11], is probably from the ^{26}Mg(n,γ) reaction. We also found no evidence in the (n,γ) reaction for the states at 3908, 5474, 6574, 6907, 6921, and 7042 keV listed in Ref. [13]. The γ rays shown there as deexciting the 3908-, 5474-, and 7042-keV levels have been assigned to the ^{25}Mg(n,γ) reaction; those deexciting the 6574-, 6907-, and 6921-keV levels were not observed.

B. Reaction ^{26}Mg$(n,\gamma)^{27}$Mg

The energies and intensities of 35 γ rays ascribed to ^{27}Mg are given in Table II(B), in addition to five γ rays for which upper intensity limits were determined. The (n,γ) level scheme (consisting of 10 excited states) is shown in Table III(B). Just as in the ^{25}Mg case, the intensity balance [see Table IV(B)] and agreement of the branching ratios with previous values [16] are both good. The two $E1$ primary transitions [see Table III(B)] of energies 2882 and 1615 keV account for 81% of the measured intensity of 39.6 mb out of the capturing state.

We have confirmed that the four γ rays assigned to ^{27}Mg in Ref. [11] and 11 out of 12 in Ref. [13] are correct. Both works employed natural magnesium targets. With an enriched target, Selin and Wallander [15] assigned 49 γ rays to ^{27}Mg, but only 13 of these were observed in the current, more sensitive work. Correspondingly, we confirm only 7 of the 11 excited states proposed in Ref. [15] as receiving significant population in the (n,γ) reaction.

TABLE II. Energies and intensities of γ rays from the reaction Mg(n,γ).

Energy[a] (keV)	Intensity[b]	Energy[a] (keV)	Intensity[b]	Energy[a] (keV)	Intensity[b]	Energy[a] (keV)	Intensity[b]
(A) Reaction ^{24}Mg$(n,\gamma)^{25}$Mg				(B) Reaction ^{26}Mg$(n,\gamma)^{27}$Mg			
389.69 *5*	7.5 *4*	2438.48 *4*	6.3 *4*	241.6 *4*	0.03 *1*	2506.57 *23*	0.15 *2*
585.06 *3*	39.8 *12*	2553.7 *8*	0.03 *1*	517.3 *3*	0.24 *3*	2576.50 *6*	1.36 *8*
611.8?	< 0.03	2563.6 *5*	0.07 *2*	713.7?	< 0.03	2655.86 *6*	1.44 *7*
836.95 *10*	0.21 *3*	2801.0 *3*	0.17 *2*	955.45 *8*	0.26 *3*	2881.67 *4*	25.6 *8*
849.9 *3*	0.07 *2*	2828.21 *4*	30.5 *10*	984.91 *3*	6.1 *3*	2887.6?	< 0.03
863.09 *5*	0.52 *5*	2972.4 *8*	0.09 *2*	1040.7?	< 0.03	2951.4 *4*	0.10 *2*
974.84 *5*	8.3 *4*	3053.99 *4*	10.4 *5*	1266.65 *18*	0.35 *3*	2966.77 *22*	0.85 *6*
989.7 *4*	0.05 *1*	3301.42 *5*	7.7 *4*	1336.80 *20*	0.17 *2*	3129.3?	< 0.03
1379.7 *3*	0.10 *2*	3413.15 *5*	5.1 *3*	1351.86 *8*	0.33 *3*	3476.19 *9*	1.17 *6*
1448.7?	< 0.03	3659.6[e] *7*	0.10 *2*	1414.95 *18*	0.17 *2*	3490.9 *6*	0.10 *2*
1474.8?	< 0.03	3691.07 *16*	0.90 *8*	1467.3 *5*	0.03 *1*	3561.31 *4*	23.5 *7*
1588.65 *9*	0.37 *4*	3916.86 *4*	41.0 *13*	1552.8 *7*	0.02 *1*	3787.05 *15*	0.69 *6*
1702.6 *7*	0.04 *1*	4141.4 *3*	0.21 *3*	1615.28 *5*	6.6 *3*	3843.01 *8*	3.14 *16*
1713.05[c] *16*	1.8 *3*	4528.47 *20*	0.46 *4*	1621.2?	< 0.03	3985.5 *6*	0.04 *1*
1964.7[d] *4*	0.06 *2*	4766.86 *23*	0.41 *4*	1698.58 *5*	1.11 *7*	4043.6 *3*	0.09 *2*
1978.25 *5*	1.42 *11*	6355.02 *10*	1.31 *9*	1792.8[f] *3*	0.03 *1*	4827.67 *6*	2.20 *13*
2213.8 *5*	0.40 *5*	6744.88 *28*	0.18 *3*	1846.95 *18*	0.26 *3*	4940.5[f] *3*	0.04 *1*
2216.5 *6*	0.25 *4*	7330.6 *9*	0.018 *4*	1862.93 *10*	0.54 *4*	5457.82 *15*	0.97 *7*
				1939.6 *4*	0.09 *2*	5924.9 *4*	0.14 *2*
				2088.66 *11*	0.41 *3*	6442.50 *6*	3.59 *17*
(C) Reaction ^{25}Mg$(n,\gamma)^{26}$Mg							
287.5 *4*	0.07 *2*	1665.39 *6*	1.22 *7*	2752.56 *25*	0.24 *4*	3611.5 *4*	0.49 *5*
347.20 *12*	0.124 *19*	1767.61 *4*	3.14 *14*	2776.82 *20*	0.51 *6*	3667.1 *9*	0.18 *4*
374.43 *8*	0.23 *3*	1774.0[f] *9*	0.79 *12*	2842.20 *12*	2.35 *13*	3672.6?	< 0.20
391.0?	< 0.03	1775.31 *5*	13.6 *5*	2865.27 *21*	1.70 *12*	3695.63 *25*	0.93 *8*
409.4[g] *5*	0.05 *1*	1779.74 *8*	1.30 *6*	2908.02 *11*	2.80 *15*	3721.4 *3*	0.77 *6*
411.3 *3*	0.070 *10*	1792.87 *12*	0.88 *8*	2911.12 *19*	1.72 *15*	3744.01 *4*	14.3 *5*
493.23 *6*	0.74 *9*	1808.68 *4*	186. *6*	2928.56 *17*	2.01 *15*	3760.0?	< 0.20
502.5 *4*	0.20 *4*	1854.5 *5*	0.24 *5*	2932.5 *4*	0.91 *10*	3783.8 *9*	0.20 *4*
730.74 *6*	1.59 *6*	1873.1 *5*	0.10 *2*	2934.8 *6*	0.42 *9*	3807.8 *9*	0.33 *6*
742.79 *12*	0.22 *4*	1896.72 *5*	9.6 *5*	2938.15 *5*	9.9 *5*	3810.13 *5*	10.1 *4*
744.0?	< 0.05	2033.88 *12*	0.59 *7*	2942.3?	< 0.20	3831.48 *4*	43.6 *14*
767.86[e] *22*	0.18 *3*	2041.44 *16*	0.47 *6*	2963.61 *9*	3.08 *22*	3847.0[e] *6*	0.44 *10*
814.3?	< 0.03	2048.2 *3*	0.21 *3*	3016.18 *23*	0.84 *8*	3882.0 *3*	0.60 *7*
833.68 *9*	0.48 *6*	2064.2[e] *5*	0.10 *3*	3021.3 *9*	0.10 *3*	3937.80 *11*	2.64 *12*
873.0 *3*	0.08 *2*	2132.71 *4*	9.4 *5*	3026.3 *6*	0.46 *6*	3993.24 *13*	1.76 *9*
966.47 *10*	0.39 *4*	2133.7[h] *9*	0.32 *5*	3029.6 *8*	0.22 *3*	4001.8 *3*	0.50 *4*
990.76 *16*	0.30 *3*	2183.83 *6*	1.87 *9*	3039.5 *8*	0.27 *4*	4030.88 *12*	1.82 *9*
1003.25 *4*	16.4 *6*	2189.59 *5*	6.16 *20*	3092.31 *11*	2.72 *20*	4122.9 *6*	0.26 *5*
1129.61 *4*	92. *3*	2264.25 *21*	0.37 *5*	3158.4 *6*	0.17 *4*	4139.7 *5*	0.28 *4*
1157.23 *6*	1.36 *10*	2290.8 *4*	0.23 *4*	3187.14 *28*	0.78 *8*	4160.96 *20*	0.91 *8*
1224.0 *3*	0.18 *3*	2353.27 *5*	4.72 *25*	3191.2 *6*	0.36 *5*	4181.9 *7*	0.23 *4*
1236.64 *5*	1.16 *5*	2381.28 *15*	0.51 *5*	3208.98 *8*	4.13 *19*	4216.38 *4*	15.0 *5*
1290.40 *7*	0.71 *6*	2387.33 *8*	1.14 *7*	3261.8 *4*	0.38 *4*	4316.39 *24*	0.66 *7*
1350.20 *16*	0.16 *3*	2410.8[e] *3*	0.14 *3*	3319.66 *5*	10.1 *4*	4322.68 *8*	3.23 *17*
1358.4 *9*	0.035 *12*	2426.09 *6*	5.34 *17*	3341.01 *7*	5.0 *4*	4332.2 *3*	0.79 *8*
1365.54 *20*	0.63 *8*	2510.01 *5*	6.0 *3*	3367.45 *22*	0.87 *6*	4346.98 *18*	0.67 *5*
1394.28 *7*	2.01 *10*	2513.52 *8*	2.93 *23*	3395.3 *7*	0.24 *3*	4355.3 *6*	0.26 *4*
1411.72 *4*	13.4 *5*	2523.69 *6*	10.4 *5*	3406.87 *22*	1.02 *9*	4410.15 *5*	7.0 *4*
1468.9[e] *3*	0.11 *3*	2541.18 *6*	14.4 *9*	3428.7 *4*	0.54 *7*	4424.2 *8*	0.22 *3*
1519.12 *5*	2.62 *10*	2543.7 *4*	0.61 *8*	3448.8 *7*	0.34 *4*	4458.43 *17*	0.94 *6*
1534.49 *15*	0.31 *4*	2557.2 *3*	0.44 *5*	3472.9 *3*	0.92 *7*	4489.4 *9*	0.22 *3*
1554.8 *4*	0.13 *2*	2560.77 *8*	1.60 *8*	3482.4 *6*	0.31 *4*	4544.5?	< 0.03
1567.06 *11*	0.46 *4*	2589.30 *8*	0.99 *6*	3500.6 *9*	0.06 *2*	4553.02 *13*	1.67 *13*
1620.8 *3*	0.35 *4*	2634.17 *13*	0.82 *6*	3551.19 *4*	11.2 *4*	4584.2?	< 0.06
1642.09 *25*	0.37 *5*	2697.7 *3*	0.40 *4*	3599.86 *14*	1.58 *10*	4602.93 *7*	3.74 *16*

TABLE II. *(Continued).*

Energy[a] (keV)	Intensity[b]	Energy[a] (keV)	Intensity[b]	Energy[a] (keV)	Intensity[b]	Energy[a] (keV)	Intensity[b]
			(C) Reaction ^{25}Mg$(n,\gamma)^{26}$Mg *(continued)*				
4834.61 *18*	1.26 *11*	5523.6 *7*	0.32 *4*	6267.0 *6*	0.28 *4*	7369.8 *7*	0.18 *3*
4886.3 *5*	0.29 *4*	5539.53 *15*	2.22 *14*	6375.38 *16*	2.04 *16*	7617.8 *7*	0.19 *3*
4891.9[e] *4*	0.20 *4*	5562.9 *9*	0.12 *3*	6386.34 *23*	0.82 *6*	7660.4 *9*	0.11 *2*
4936.3 *3*	0.66 *6*	5593.2 *4*	0.35 *4*	6417.9 *3*	0.67 *8*	7695.6 *8*	0.10 *2*
4961.42 *22*	1.57 *12*	5616.8 *3*	0.54 *5*	6441.1 *8*	0.069 *14*	7807.0 *9*	0.10 *2*
4967.19 *4*	17.0 *6*	5632.3 *6*	0.24 *3*	6488.6 *4*	0.57 *5*	8153.54 *5*	29.8 *10*
4975.3 *9*	0.26 *4*	5691.1 *9*	0.05 *2*	6649.1 *7*	0.15 *3*	8225.6 *4*	0.43 *4*
4992.4 *8*	0.39 *5*	5732.37 *15*	1.72 *13*	6657.3 *5*	0.24 *4*	8316.4 *8*	0.23 *3*
5020.7 *8*	0.20 *3*	5766.6 *3*	0.65 *6*	6694.0 *7*	0.22 *3*	8409.7 *9*	0.11 *2*
5067.13 *4*	10.1 *4*	5800.69 *9*	3.15 *12*	6722.1 *7*	0.16 *3*	8502.2 *3*	0.65 *5*
5077.4 *9*	0.13 *4*	5915.8 *9*	0.10 *3*	6742.21 *7*	4.21 *16*	8539.2 *9*	0.10 *2*
5223.37 *12*	1.64 *14*	5924.8 *9*	0.11 *2*	6759.73 *11*	2.29 *15*	8552.2 *3*	0.61 *6*
5245.9 *3*	0.56 *7*	5964.31 *20*	0.59 *5*	6773.1 *3*	0.69 *5*	8957.7 *5*	0.32 *3*
5252.9 *3*	0.55 *6*	5975.3[e] *7*	0.08 *2*	7054.0 *6*	0.16 *2*	8996.5 *9*	0.04 *1*
5290.3 *5*	0.29 *4*	6011.2 *5*	0.30 *4*	7060.6 *7*	0.097 *19*	9237.1 *8*	0.14 *2*
5291.1 *5*	0.18 *3*	6104.3 *9*	0.13 *3*	7098.9 *5*	0.10 *3*	9282.68 *6*	4.55 *16*
5311.66 *16*	1.77 *11*	6120.1 *4*	0.50 *4*	7150.61 *7*	2.29 *14*	9854.5 *7*	0.14 *3*
5376.1 *8*	0.13 *3*	6191.11 *25*	0.53 *4*	7162.4 *9*	0.08 *2*	10100.5 *4*	0.23 *3*
5383.8 *7*	0.13 *3*	6242.9 *7*	0.25 *3*	7187.4 *8*	0.12 *2*	11090.7 *7*	0.28 *4*
5401.3 *4*	0.45 *4*	6249.7 *9*	0.09 *2*	7260.3?	< 0.03		
5452.03 *4*	21.3 *7*	6257.1 *3*	0.68 *5*	7347.7?	< 0.03		

[a]In our notation, 389.69 *5* is 389.69±0.05 keV, etc. A question mark following a transition denotes an expected transition for which an upper limit in intensity was determined.
[b]γ-ray cross section in mb. Multiply by 1.85, 2.56, and 0.50 to obtain photons per 100 thermal neutron captures by ^{24}Mg, ^{26}Mg, and ^{25}Mg, respectively. In our notation 7.5 *4* is 7.5±0.4, etc.
[c]Interference from the single-escape peak of the 2223-keV γ ray in ^{2}H.
[d]Interference from Gd(n,γ).
[e]γ ray not placed on the level scheme.
[f]Presence deduced from the known level energies and branching ratios.
[g]γ ray placed twice on the level scheme.
[h]Inferred from the intensity balance requirements for the 8959.4-keV level.

C. Reaction ^{25}Mg$(n,\gamma)^{26}$Mg

The energies and intensities of 212 γ rays assigned to ^{26}Mg are given in Table II(C) in addition to 10 γ rays for which upper intensity limits were obtained. Of these 212 γ rays, 205 have been placed in a scheme [see Table III(C)] consisting of 55 excited states. Only two of these levels (at 10 220 and 10 806 keV) remain uncorroborated by any reaction experiment (see Ref. [16]). For levels that are common, our branching ratios are generally consistent with those given by Endt [16] and those determined in the ^{23}Na$(\alpha,p\gamma)$ study by Glatz *et al.* [17]. (However, the 6876→3942 branch was found to be only 3% instead of 20% given in Ref. [16], and the 7349→0 branch with a reported intensity of 23±5% [16] was not observed at the 0.3% level.) The intensities out of the known levels at 10 682, 10 719, and 10 746 keV [see Table IV(C)] are probably fractionated so that the corresponding secondary γ rays fall below our detection limits. These three levels and the one at 10 806 keV are also slightly above the ^{22}Ne+α threshold energy of 10 612 keV.

Compared to our leve scheme of 55 levels and 205 transitions, that proposed by Kennett and Prestwich [13] consists of 48 levels and 114 transitions. We agree on 35 levels, but find no evidence for the remaining 13 levels proposed in Ref. [13] at 7249, 7397, 7428, 7692, 7771, 7828, 8196, 8201, 8467, 8554, 9462, 9843, and 9894 keV. The γ rays associated with these levels in Ref. [13] are either not seen in our work with an enriched target, or placed as different transitions, or identified as impurity lines, or attributed to decays in a different magnesium isotope. (The 9462-keV level listed in Table 7 of Ref. [13] has *no* γ ray associated with it in that paper.)

The neutron-capturing state in ^{26}Mg is a $2^+ + 3^+$ mixture. The strongest of all primary transitions [see Table III(C)], the one at 3831 keV with an intensity of 43.6 mb, is an $E1$ transition. This and six other definite primary $E1$ transitions account for 49% of the total capture cross section of ~200 mb. The second strongest of all primary transitions, the one at 8154 keV with an intensity of 29.8 mb, is an $M1$ transition. This and 19 other definite primary $M1$ transitions account for 36% of the total capture cross section. There are also two definite primary $E2$ transitions, at 6120 (0.50 mb) and 11 091 (0.28 mb) keV, accounting for ~0.4%.

Wildenthal [18] has carried out shell-model calculations for ^{26}Mg and ^{26}Al in the full *sd* space with 10 nu-

TABLE III. Level schemes of Mg isotopes in tabular form.

Level energy[a] (keV)	Deexciting γ rays[b] (keV)	Level energy[a] (keV)	Deexciting γ rays[b] (keV)
	(A) Levels in ^{25}Mg		(B) Levels in ^{27}Mg
0.0		0.0	
585.07 *3*	585.06	984.92 *3*	984.91
974.81 *3*	974.84, 389.69	1698.63 *5*	1698.58, 713.7?
1964.66 *14*	1964.7, 1379.7, 989.7	1940.35 *8*	1939.6, 955.45, 241.6
2563.43 *5*	2563.6, 1978.25, 1588.65	3476.33 *6*	3476.19
2801.61 *14*	2801.0, 2216.5, 836.95	3491.47 *13*	3490.9, 2506.57, 1792.8
3413.43 *3*	3413.15, 2828.21, 2438.48, 1448.7?, 849.9, 611.8?	3561.56 *3*	3561.31, 2576.50, 1862.93, 1621.2?
		3787.38 *6*	3787.05, 2088.66, 1846.95
4276.48 *4*	3691.07, 3301.42, 1713.05, 1474.8?, 863.09	4828.14 *4*	4827.67, 3843.01, 3129.3?, 2887.6?, 1351.86, 1336.80, 1266.65, 1040.7?
4358.1 *8*			
5116.62 *24*	4141.4, 2553.7, 1702.6	5028.58 *15*	4043.6, 1552.8, 1467.3
7330.65[c] *4*	7330.6, 6744.88, 6355.02, 4766.86, 4528.47, 3916.86, 3053.99, 2972.4, 2213.8	5925.93 *18*	5924.9, 4940.5, 3985.5
		6443.40[c] *4*	6442.50, 5457.82, 2966.77, 2951.4, 2881.67, 2655.86, 1615.28, 1414.95, 517.3

(C) Levels in ^{26}Mg

0.0		8458.87 *13*	6649.1, 4139.7
1808.74 *4*	1808.68	8503.74 *9*	8502.2, 6694.0
2938.33 *4*	2938.15, 1129.61	8532.27 *9*	6722.1, 5593.2, 4181.9
3588.56 *9*	1779.74	8705.73 *9*	5766.6, 4355.3
3941.55 *4*	2132.71, 1003.25	8863.8 *5*	7054.0, 5924.8, 4544.5?
4318.88 *6*	2510.01	8903.50 *6*	5964.31, 4961.42, 4584.2?, 4553.02, 4001.8, 3611.5, 1642.09, 1620.8, 1554.8
4332.57 *5*	4332.2, 2523.69, 1394.28, 744.0?, 391.0?		
4350.08 *5*	2541.18, 1411.72, 409.4	8959.4 *5*	8957.7
4835.13 *5*	4834.61, 3026.3, 1896.72, 502.5	9044.7 *3*	6104.3
4901.30 *9*	3092.31	9238.7 *5*	9237.1
4972.29 *12*	2033.88	9325.51 *6*	6386.34, 5383.8, 4992.4, 4975.3, 4489.4, 4424.2
5291.74 *5*	5291.1, 3482.4, 2353.27, 1350.20		
5476.11 *7*	3667.1, 1534.49, 1157.23	9427.74 *7*	7617.8, 6488.6, 5077.4
5691.11 *17*	5691.1, 3882.0, 2752.56, 1358.4	9574.02 *6*	5632.3, 5223.37, 3448.8, 2697.7, 2290.8
5715.60 *10*	2776.82, 1774.0, 1365.54, 814.3?	9617.0 *9*	7807.0
6125.48 *4*	4316.39, 3187.14, 2183.83, 1792.87, 1775.31, 1290.40, 1224.0, 833.68, 409.4	9856.52 *6*	9854.5, 5915.8, 5523.6, 5020.7
		10102.41 *15*	10100.5, 7162.4
6634.31 *15*	3695.63	10126.70 *10*	8316.4, 7187.4
6745.76 *16*	4936.3, 3807.8	10220.1 *3*	8409.7
6876.42 *4*	5067.13, 3937.80, 2934.8, 2557.2, 2543.7, 2041.44	10350.37 *12*	8539.2
		10362.42 *7*	8552.2, 6011.2, 4886.3, 3261.8
7061.90 *10*	7060.6, 5252.9, 4122.9, 3472.9	10599.96 *7*	7660.4, 6657.3, 6267.0, 6249.7, 3500.6
7099.66 *10*	7098.9, 5290.3, 4160.96, 3158.4, 2264.25	10681.9 *3*	
7261.39 *4*	7260.3?, 5452.03, 4322.68, 3672.6?, 3319.66, 2942.3?, 2928.56, 2911.12, 2426.09	10718.75 *9*	
		10745.98 *12*	
7282.74 *5*	3341.01, 2963.61, 2932.5, 2381.28, 1567.06	10805.9 *4*	8996.5
7348.87 *5*	7347.7?, 5539.53, 4410.15, 3760.0?, 3029.6, 3016.18, 2513.52, 1873.1	11093.18[c] *3*	11090.7, 9282.68, 8153.54, 7150.61, 6773.1, 6759.73, 6742.21, 6257.1, 6191.11, 6120.1, 5800.69, 5616.8, 5401.3, 5376.1, 4967.19, 4458.43, 4346.98, 4216.38, 4030.88, 3993.24, 3831.48, 3810.13, 3744.01, 3721.4, 3551.19, 3395.3, 3367.45, 3039.5, 2908.02, 2865.27, 2842.20, 2634.17, 2589.30, 2560.77, 2387.33, 2189.59, 2133.7, 2048.2, 1854.5, 1767.61, 1665.39, 1519.12, 1236.64, 990.76, 966.47, 873.0, 742.79, 730.74, 493.23, 411.3, 374.43, 347.20, 287.5
7371.20 *22*	7369.8, 5562.9, 3428.7, 3021.3		
7541.73 *5*	5732.37, 4602.93, 3599.86, 3208.98, 3191.2		
7697.3 *6*	7695.6		
7725.74 *16*	3783.8, 3406.87		
8052.9 *6*	6242.9		
8184.96 *10*	6375.38, 5245.9		
8227.56 *16*	8225.6, 6417.9		
8250.70 *10*	6441.1, 5311.66		

[a]In our notation, 585.073 *25* is 585.073 ± 0.025 keV, etc.
[b]See Table II for the intensity values. A question mark following a γ ray denotes an expected transition for which an upper intensity limit was determined. For some levels in ^{25}Mg and ^{26}Mg fed by primary γ rays, no deexciting γ rays were observed.
[c]Capturing state.

TABLE IV. Intensity balance in the reaction Mg(n,γ).

E(level) (keV)	J^{π} [a]	ΣI_γ(in) (mb)	ΣI_γ(out) (mb)	ΣI_γ(net) (mb)	E(level) (keV)	J^{π} [a]	ΣI_γ(in) (mb)	ΣI_γ(out) (mb)	ΣI_γ(net) (mb)
	(A) Reaction ^{24}Mg$(n,\gamma)^{25}$Mg					(B) Reaction ^{26}Mg$(n,\gamma)^{27}$Mg			
0.0	$\frac{5}{2}^+$	53.5 *13*		53.5 *13*	0.0	$\frac{1}{2}^+$	38.7 *8*		38.7 *8*
585.07 *3*	$\frac{1}{2}^+$	40.9 *11*	39.8 *12*	1.1 *17*	984.92 *3*	$\frac{3}{2}^+$	6.0 *2*	6.1 *3*	−0.1 *4*
974.81 *3*	$\frac{3}{2}^+$	15.9 *6*	15.8 *6*	0.1 *8*	1698.63 *5*	$\frac{5}{2}^+$	1.01 *6*	1.11 *7*	−0.10 *9*
1964.66 *14*	$\frac{5}{2}^+$	0.21 *3*	0.21 *3*	0.00 *5*	1940.35 *8*	$\frac{5}{2}^+$	0.30 *4*	0.38 *4*	−0.08 *5*
2563.43 *5*	$\frac{1}{2}^+$	2.3 *3*	1.86 *12*	0.5 *4*	3476.33 *6*	$\frac{1}{2}^+$	1.20 *7*	1.17 *6*	0.03 *9*
2801.61 *14*	$\frac{3}{2}^+$	0.46 *4*	0.63 *6*	−0.17 *7*	3491.47 *13*	$\frac{3}{2}^+, \frac{5}{2}^+$	0.27 *3*	0.28 *3*	−0.01 *5*
3413.43 *3*	$\frac{3}{2}^-$	41.6 *13*	42.0 *12*	−0.4 *18*	3561.56 *3*	$\frac{3}{2}^-$	26.0 *8*	25.4 *7*	0.6 *11*
4276.48 *4*	$\frac{1}{2}^-$	10.4 *5*	10.9 *5*	−0.5 *8*	3787.38 *6*	$\frac{3}{2}^+$	1.44 *7*	1.36 *8*	0.08 *11*
4358.1 *8*	$\frac{3}{2}^+$	0.09 *2*		0.09 *2*	4828.14 *4*	$\frac{1}{2}^-, \frac{3}{2}^-$	6.6 *3*	6.2 *3*	0.4 *4*
5116.62 *24*	$\frac{1}{2}^-$	0.40 *5*	0.28 *4*	0.12 *6*	5028.58 *15*	$\frac{1}{2}^+$	0.17 *2*	0.14 *3*	0.03 *4*
7330.65[b] *4*	$\frac{1}{2}^+$		54.3 *14*	−54.3 *14*	5925.93 *18*		0.24 *3*	0.22 *3*	0.02 *4*
					6443.40[b] *4*	$\frac{1}{2}^+$		39.6 *9*	−39.6 *9*
	(C) Reaction ^{25}Mg$(n,\gamma)^{26}$Mg								
0.0	0^+	201 *6*		201 *6*	8184.96 *10*		2.80 *15*	2.60 *18*	0.20 *23*
1808.74 *4*	2^+	185 *4*	186 *6*	−1 *7*	8227.56 *16*	$(1,2^+)$	1.70 *12*	1.10 *9*	0.60 *15*
2938.33 *4*	2^+	103 *2*	102 *3*	1 *4*	8250.70 *10*	1^-	2.35 *13*	1.84 *11*	0.51 *17*
3588.56 *9*	0^+	0.92 *7*	1.30 *6*	−0.38 *10*	8458.87 *13*		0.82 *6*	0.43 *5*	0.39 *8*
3941.55 *4*	3^+	25.8 *7*	25.8 *8*	0.0 *10*	8503.74 *9*		0.99 *6*	0.87 *6*	0.12 *9*
4318.88 *6*	4^+	7.1 *3*	6.0 *3*	1.1 *4*	8532.27 *9*		1.60 *8*	0.74 *7*	0.86 *11*
4332.57 *5*	2^+	12.0 *4*	13.2 *6*	−1.2 *7*	8705.73 *9*	(2^+-4^+)	1.14 *7*	0.91 *8*	0.23 *10*
4350.08 *5*	3^+	26.1 *6*	27.9 *11*	−1.7 *12*	8863.8 *5*	2^+		0.27 *3*	−0.27 *3*
4835.13 *5*	2^+	10.9 *3*	11.5 *6*	−0.6 *6*	8903.50 *6*		6.16 *20*	5.67 *21*	0.5 *3*
4901.30 *9*	4^+	1.9 *1*	2.7 *2*	−0.8 *2*	8959.4 *5*		0.32 *5*	0.32 *3*	0.00 *6*
4972.29 *12*	0^+	0.50 *4*	0.59 *7*	−0.09 *8*	9044.7 *3*		0.21 *3*	0.13 *3*	0.08 *5*
5291.74 *5*	2^+	4.1 *2*	5.4 *3*	−1.2 *3*	9238.7 *5*	1^+	0.24 *5*	0.14 *2*	0.10 *6*
5476.11 *7*	4^+	0.93 *7*	1.85 *12*	−0.92 *14*	9325.51 *6*		3.14 *14*	2.04 *11*	1.10 *18*
5691.11 *17*	1	0.45 *4*	0.93 *9*	−0.48 *10*	9427.74 *7*		1.22 *7*	0.89 *7*	0.33 *10*
5715.60 *10*	4^+	0.64 *5*	1.93 *16*	−1.29 *17*	9574.02 *6*		2.62 *10*	2.85 *16*	−0.23 *19*
6125.48 *4*	3^+	17.3 *6*	19.2 *6*	−1.9 *8*	9617.0 *9*			0.10 *2*	−0.10 *2*
6634.31 *15*	(2^+-4^+)	0.94 *6*	0.93 *8*	0.01 *10*	9856.52 *6*	2^+	1.16 *5*	0.76 *7*	0.40 *9*
6745.76 *16*	2^+	0.67 *5*	0.99 *9*	−0.32 *10*	10102.41 *15*		0.30 *3*	0.31 *4*	−0.01 *5*
6876.42 *4*	3^-	15.4 *5*	14.7 *5*	0.7 *7*	10126.70 *10*	4^+	0.39 *4*	0.35 *4*	0.04 *6*
7061.90 *10*	1^-	1.82 *9*	1.83 *11*	−0.01 *14*	10220.1[c] *3*		0.08 *2*	0.11 *2*	−0.03 *3*
7099.66 *10*	2^+	2.20 *10*	1.84 *12*	0.36 *16*	10350.37 *12*		0.22 *4*	0.10 *2*	0.12 *5*
7261.39 *4*	$(2,3)^-$	44.0 *14*	43.7 *9*	0.3 *17*	10362.42 *7*		1.59 *6*	1.58 *10*	0.01 *11*
7282.74 *5*	4^-	10.7 *4*	10.0 *5*	0.7 *7*	10599.96 *7*		0.74 *9*	0.78 *7*	−0.04 *12*
7348.87 *5*	3^-	14.4 *5*	13.3 *5*	1.1 *7*	10681.9 *3*		0.07 *1*		0.07 *1*
7371.20 *22*	$(1,2)^+$	0.77 *6*	0.94 *9*	−0.17 *11*	10718.75 *9*		0.23 *3*		0.23 *3*
7541.73 *5*	$(2,3)^-$	11.2 *4*	11.5 *3*	−0.3 *5*	10745.98 *12*		0.12 *2*		0.12 *2*
7697.3 *6*	$(1,2^+)$	0.24 *3*	0.10 *2*	0.14 *4*	10805.9[c] *4*		0.07 *2*	0.04 *1*	0.03 *2*
7725.74 *16*	$(2-5)^+$	0.87 *6*	1.22 *10*	−0.35 *12*	11093.18[b] *3*	$2^+ + 3^+$		199 *3*	−199 *3*
8052.9 *6*	2^+	0.27 *4*	0.25 *3*	0.02 *5*					

[a]Spin and parity assignments from Ref. [16].
[b]Capturing state.
[c]Proposed new level.

cleons in the $1d_{5/2}$, $2s_{1/2}$, and $1d_{3/2}$ orbits. The relevant details and results have been published [19]. The excellent correspondence between the ^{26}Mg levels, the calculated levels of ^{26}Mg, and the $T=1$ levels of ^{26}Al has also been noted in Ref. [19].

D. Neutron separation energies

The measured neutron separation energies (see Table IV) for ^{25}Mg, ^{27}Mg, and ^{26}Mg are, respectively, 7330.65±0.05, 6443.40±0.05, and 11 093.16±0.05 keV, where the uncertainty now includes the uncertainty in the primary calibration energies. The $S_n(^{26}\mathrm{Mg})=11\,093.18\pm0.05$-keV value reported here is slightly *lower* than the value 11 093.24±0.06 keV reported by us in a recent paper [20] on the superallowed $^{26}\mathrm{Al}^m\rightarrow{}^{26}\mathrm{Mg}$ decay. This change is due to two factors: (1) We have reevaluated the nonlinearity of our system and (2) the primary calibration energies that were used in Ref. [20] have since been revised *downwards*—$S_n(^2\mathrm{H})$ by 3 eV, $S_n(^{13}\mathrm{C})$ by 24 eV, and $S_n(^{15}\mathrm{N})$ by 70 eV—by Wapstra [8].

E. Capture cross sections

If a level scheme is complete and internal conversion can be neglected, the three quantities $\sum I_\gamma$ (primary), $\sum E_\gamma I_\gamma/S_n$, and $\sum I_\gamma$ (secondary to the ground state) should all be the same within their stated uncertainties. For the $^{24}\mathrm{Mg}(n,\gamma)$ reaction, the measured values (in mb) are 54.3±1.4, 54.7±1.4, and 53.5±1.3, respectively, leading to an adopted value of 54.1±1.3 mb for this cross section, which is significantly more precise than the currently accepted value of 51±5 mb [10]. In the case of the $^{26}\mathrm{Mg}(n,\gamma)$ reaction, we also have a fourth quantity, namely, $\sum I_\gamma$ (feeding to the ^{27}Al ground state) following the β^- decay of ^{27}Mg to ^{27}Al. The corresponding measured values are 39.6±0.9, 38.8±0.9, 38.7±0.8, and 39.2±1.0 (the last one from decay), leading to an adopted value of 39.0±0.8 mb, which is in excellent agreement with 38.2±0.8 mb reported by Ryves [21] (and adopted in Ref. [10]) via activation measurements. Finally, the three relevant quantities from the $^{25}\mathrm{Mg}(n,\gamma)$ reaction have the values 199±3, 200±3, and 201±6, respectively, leading to a final value of 200±3 mb for this cross section, compared to 190±30 mb in Ref. [10].

F. Other relevant data

For the theoretical analysis of the capture data, we require knowledge of the free nuclear scattering lengths a and final-state (d,p) spectroscopic strengths ($l=1$ and $l=0$ strengths, respectively, for the analyses of $E1$ and $M1$ transitions) for the different magnesium isotopes. The a values have recently been compiled by Koester, Rauch, and Seymann [22]. The (d,p) strengths (see Tables V and VI) for levels in ^{25}Mg were obtained from Refs. [23] and [24], for ^{27}Mg from Ref. [25], and for ^{26}Mg from Refs. [26] and [27].

IV. PRIMARY ELECTRIC-DIPOLE TRANSITIONS

We have calculated the cross sections for the main primary $E1$ transitions of the three stable magnesium isotopes from the data on final-state excitation energies, spectroscopic strengths, and scattering lengths, using the $G+V$ and S methods described in Refs. [2–4]. As with other nuclides that we have studied [1–6], we find that the two approaches give very similar results (within a few percent). Hence, we quote here in Table V only the results from the $G+V$ method alongside the data. The implied compound-nuclear contribution to the capture cross section from the discrepancies between theory and experiment is also shown in the last column of this table.

For all three targets, it is apparent by comparing the $\sigma(G+V)$ and $\sigma_\gamma(X)$ columns of Table V that the results of the direct-capture theory are in reasonable overall agreement (within a factor of ~2) with the data. In the case of ^{24}Mg [see Table V(A)] the theoretical estimates for the 3917- and 3054-keV transitions are smaller than the measured values, but the resulting hypothesized compound-nuclear component, averaged for these two and the 2214-keV transition, is quite small, namely, $\langle\Gamma_{\gamma,\mathrm{CN}}/E_\gamma^3\rangle/E_\gamma\approx-21\times10^{-9}$ MeV^{-3}, which is larger than the Cameron [28] statistical estimate of compound radiation strength $\langle\Gamma_{\gamma,\mathrm{CN}}/E_\gamma^3\rangle/D\approx2.7\times10^{-9}$ MeV^{-3}, indicating that the local resonance level E_γ mainly responsible for this component is bound by about $\frac{1}{8}$ of the mean level spacing D.

In the case of ^{25}Mg [see Table V(C)] the theoretical values are scattered more randomly about the data, and here again the inferred compound-nuclear component is physically reasonable. Because the experimental $J=2$ scattering length, $a_{J=2}(X)=2.60$ fm, deviates significantly from the calculated potential-scattering length, $a(G)=4.29$ fm, it is reasonable to assume that most of the capture is due to the $J=2$ initial state. With this assumption, we find that $\langle\Gamma_{\gamma,\mathrm{CN}}/E_\gamma^3\rangle/E_\gamma\approx30\times10^{-9}$ MeV^{-3}. Thus we expect that a single local level should be found at about $\frac{1}{10}$ of the average spacing of 2^+ resonances, which is 50–100 keV. The first known 2^+ resonance is in fact at 19.9 keV, a little higher than expected, but not unduly so considering the very meager statistics we have on the average compound-nuclear radiation width (four transitions out of a Porter-Thomas distribution). The 19.9-keV reosnance has a reduced neutron width (the resonance neutron width divided by the square root of the resonance energy) of $\Gamma_n^0\approx12.7$ eV$^{1/2}$, giving $\Gamma_n^0/E_\gamma\approx6.4\times10^{-4}$ eV$^{1/2}$, which is close to the value implied by the difference between the experimental scattering length and the potential-scattering length.

In the case of the $^{26}\mathrm{Mg}(n,\gamma)$ reaction [see Table V(B)], the theoretical cross sections for the four listed primary $E1$ transitions are larger than the experimental values. The extracted estimate of $\langle\sigma_{\mathrm{CN},\gamma}/E_\gamma^3\rangle$ is dominated by the 534-keV transition to the 5909-keV state. Because of this one low-energy transition, the modulus value of $\approx-300\times10^{-9}$ MeV^{-3} for $\langle\Gamma_{\gamma,\mathrm{CN}}/E_\gamma^3\rangle/E_\gamma$ is an order of magnitude greater than for the other two isotopes.

TABLE V. Direct-capture cross sections for primary $E1$ transitions in the reaction Mg(n,γ) with enriched isotopes. Columns 1, 2, and 3 give the energy, J^π value, and the $\ell=1$ (d,p) spectroscopic factor multiplied by $(2J+1)$ for the final state, respectively. Column 4 is the primary transition energy. Column 5 is the average valency capture width and column 6 the potential capture cross section, both calculated using a global optical potential (see Eqs. (4)–(7) of Ref. [3]). The entries in column 5 do not include the spin-coupling factor and the spectroscopic factor; those in column 6 do. Column 7 is the calculated cross section using the global plus valence $(G+V)$ procedure. The measured cross sections are given in column 8. Finally, column 9 gives the hypothesized compound-nuclear contributions deduced from the differences between column 7 and column 8 via Eq. (8) of Ref. [3]. In the table subheading, $a(X)$ refers to the experimental scattering length, while $a(G)$ and $\overline{\Gamma_n^0}/D$ refer to the scattering length and the neutron strength function, respectively, both calculated using the global optical potential.

E_f (keV)	J^π	(d,p) $(2J+1)S^a$	E_γ (keV)	$\Gamma_{\gamma,\mathrm{val}}/DE_\gamma^3$ $(10^{-7}\mathrm{MeV}^{-3})$	$\sigma_{\mathrm{pot},\gamma}$ (mb)	$\sigma(G+V)$ (mb)	$\sigma_\gamma(X)$ (mb)	$\sigma_{\mathrm{CN},\gamma}$ (mb)
	(A) Reaction ^{24}Mg$(n,\gamma)^{25}$Mg; $a(X)=5.27$ fm; $a(G)=4.35$ fm; $\overline{\Gamma_n^0}/D=8.35\times10^{-5}$							
3413	$\frac{3}{2}^-$	1.06	3917	0.485	40.3	18.3	41.0 *13*	4.5
4276	$\frac{1}{2}^-$	0.40	3054	0.528	10.5	5.4	10.4 *5*	0.8
5116	$\frac{1}{2}^-$	0.028	2214	0.773	0.59	0.35	0.40 *5*	≤ 0.002
	(B) Reaction ^{26}Mg$(n,\gamma)^{27}$Mg; $a(X)=4.71$ fm; $a(G)=4.22$ fm; $\overline{\Gamma_n^0}/D=7.55\times10^{-5}$							
3562	$\frac{3}{2}^-$	1.6	2882	0.529	48.3	36.1	25.6 *8*	0.9
4828	if $\frac{1}{2}^-$ if $\frac{3}{2}^-$	0.64 0.62	1615	0.879 1.010	10.1 11.7	8.2 9.5	6.6 *3*	0.1 0.3
	$\frac{1}{2}^-$	0.008		1.424	0.09	0.08	< 0.04	≤ 0.08
5909	if $\frac{1}{2}^-$ if $\frac{3}{2}^-$	0.046	534	2.821 3.103	0.26 0.29	0.24 0.26	< 0.03	≤ 0.24 ≤ 0.26
	(C) Reaction ^{25}Mg$(n,\gamma)^{26}$Mg; $a_{J=2}(X)=2.60$ fm; $a_{J=3}(X)=4.42$ fm; $a(G)=4.29$ fm; $\overline{\Gamma_n^0}/D=7.90\times10^{-5}$							
6876	3^-	1.18	4216	0.395 if $j=\frac{3}{2}$ 0.313 if $j=\frac{1}{2}$	7.8 6.2	12.8 11.5	15.0 *5*	0.09 0.23
7261	if 2^- if 2^- if 3^- if 3^-	1.48	3832	0.443 if $j=\frac{3}{2}$ 0.356 if $j=\frac{1}{2}$ 0.443 if $j=\frac{3}{2}$ 0.356 if $j=\frac{1}{2}$	9.2 7.3 9.2 7.3	19.6 9.3 14.9 13.2	43.6 *14*	4.7 12.6 7.5 8.8
7349	3^-	1.14	3744	0.455 if $j=\frac{3}{2}$ 0.367 if $j=\frac{1}{2}$	5.0 4.0	11.2 10.0	14.3 *5*	0.2 0.4
7542	if 2^- if 2^- if 3^- if 3^-	0.36	3551	0.484 if $j=\frac{3}{2}$ 0.392 if $j=\frac{1}{2}$ 0.484 if $j=\frac{3}{2}$ 0.392 if $j=\frac{1}{2}$	1.5 1.2 1.5 1.2	4.4 2.2 3.3 3.0	11.2 *4*	1.6 3.5 2.3 2.6

[a]The strengths for the 3413- and 4276-keV levels in ^{25}Mg are averages of the values given in Refs. [23] and [24], and that for the 5116-keV level is from Ref. [24]. The strengths for levels in ^{27}Mg and ^{26}Mg are from Refs. [25] and [26], respectively. In Ref. [26], the bulk of the $\ell=1$ strength in the unresolved 7261–7281 doublet has been assigned to the 7261-keV level.

This result suggests a very weakly bound level with a small reduced neutron width.

V. PRIMARY MAGNETIC-DIPOLE TRANSITIONS

Several primary $M1$ transitions have been observed in this work. In the capture by the two even magnesium isotopes, these are 1–2 orders of magnitude weaker than the $E1$ transitions, but for capture by ^{25}Mg, they are almost as strong as the $E1$ transitions. In this section we speculate on the mechanism for the $M1$ transitions.

Some tendency (see Table VI) for the strong $M1$ transitions to be associated with high spectroscopic factors for the final states suggests the operation of a direct mechanism quite analogous to that for $E1$ transitions. In this case, the chances of a successful theory are slimmer for two reasons. The first is that in the $E1$ case the matrix elements are concerned with the electrostatic dipole moment, whereas in the $M1$ case, the operator depends on currents that may be described much more poorly by the wave functions of a simple direct-capture model. The second reason is that the radial component of the $E1$ matrix element is more strongly weighted to the channel region—where the wave functions are well established by the energies of the initial and final states—than is the radial $M1$ element. In fact, in the $M1$ case, it is often stated that there can be no direct capture analogous to $E1$ because the radial wave functions are necessarily orthogonal in a simple potential well. However, because of the complexity of the nucleus, we usually find it necessary to generate the radial wave functions of the initial and final states with rather different potentials (just as we usually do for $E1$ capture) and $M1$ transitions become possible.

The $M1$ operator has the simple form [6]

TABLE VI. Direct-capture cross sections for primary $M1$ transitions in the reaction Mg(n,γ) with enriched isotopes. Columns 1, 2, and 3 give the energy, J^π value, and the $\ell = 0$ (d,p) spectroscopic factor multiplied by $(2J+1)$ for the final state, respectively. Column 4 is the primary transition energy. The measured cross sections are given in column 5. Column 6 contains the calculated cross sections according to the direct-capture theory adapted for $M1$ transitions.

E_f (keV)	J^π	(d,p) $(2J+1)S^a$	E_γ (keV)	$\sigma_\gamma(X)$ (mb)	σ_γ(theory) (mb)
		(A) Reaction ^{24}Mg$(n,\gamma)^{25}$Mg			
585	$\frac{1}{2}^+$	0.84	6745	0.18 *3*	0.285
2563	$\frac{1}{2}^+$	0.30	4767	0.41 *4*	0.001
5465	$\frac{1}{2}^+$	0.34	1866	< 0.03	0.036
		(B) Reaction ^{26}Mg$(n,\gamma)^{27}$Mg			
0	$\frac{1}{2}^+$	1.5	6442	3.59 *17*	0.041
3476	$\frac{1}{2}^+$	0.58	2967	0.85 *6*	0.164
5029	$\frac{1}{2}^+$	0.048	1415	0.17 *2*	0.010
		(C) Reaction ^{25}Mg$(n,\gamma)^{26}$Mg			
1809	2^+	0.17	9283	4.55 *16*	0.005
2938	2^+	2.65	8154	29.8 *10*	0.078
3942	3^+	1.86	7151	2.29 *14*	0.715
4835	2^+	0.30	6257	0.68 *5*	0.013
6125	3^+	0.80	4967	17.0 *6*	0.241
6746	2^+	0.04	4347	0.67 *5*	0.002
7815	$(2,3)^+$	0.62	3278	< 0.04	0.036

[a]The strengths for levels in ^{25}Mg are averages of the values given in Refs. [23] and [24], those in ^{27}Mg are from Refs. [25], and those in ^{26}Mg are averages of the values given in Refs. [26] and [27].

$$H'_{M1,\mathcal{M}} = \frac{e\hbar}{2mc}\left[\frac{3}{4\pi}\right]^{1/2}\left[\frac{\mu_I \mathbf{I}_{\mathcal{M}}}{\mathbf{I}} + \frac{\mu_n \sigma_{n,\mathcal{M}}}{\sigma}\right], \quad (1)$$

where e is the proton charge, m the nucleon mass, c the velocity of light, μ_I (μ_n) the magnetic moment (in units of nuclear magnetons μ_0) of the target nucleus (neutron), $\mathbf{I}$ the target-nucleus spin operator, and σ the Pauli spin operator for the neutron. From this expression the reduced matrix element for the spin factor can be computed, while the radial matrix element is simply the integral of the product of the projection of the radial wave function of the initial state onto the entrance channel (see Ref. [1]) and the radial wave function of the single-particle component of the final state. Because there is no orbital contribution in the above $M1$ operator, the single-particle components of the initial and final states have zero orbital angular momentum in slow-neutron direct $M1$ capture.

The calculated values of the direct-capture cross sections for $M1$ primary transitions to final states with $l=0$ stripping patterns are shown in Table VI along with the experimental cross sections and other relevant data. It is apparent that on the average the theory fails to explain the measurements by about 2 orders of magnitude. This is true even for the lowest-energy transitions, except possibly for the 1866-keV transition in ^{25}Mg and the 3278-keV transition in ^{26}Mg.

Setting aside the direct-capture theory, it does seem that the high-energy transitions may be explainable semiquantitatively as a consequence of the giant magnetic-dipole reosnance [29]. Just as in the Brink model [30] for $E1$ transitions, we assume that a giant $M1$ resonance (with properties similar to those governing transitions from the ground state) is available for every final state reached in transitions from the compound state. In the magnesium isotopes, the $M1$ resonance involves mainly the $1d_{5/2}$ and $1d_{3/2}$ shell-model orbits. The single-particle $1d_{5/2} \rightarrow 1d_{3/2}$ transition energy is expected to be ~ 5 MeV, but with collective coupling, the giant-resonance energy could be in the region of 11 MeV [29]. We assume that the giant-resonance mechanism would have to occur through the agency of a resonance level for which we assign a Γ_n^0/E_γ value that is deduced from the difference between the observed and calculated (potential) scattering lengths. Thus, given an $M1$ giant resonance at 11 MeV with a radiation width of 100 eV (using the parameters of Ref. [29]) and an assumed damping width of 2 MeV, we estimate ~ 0.4 and ~ 0.065 mb for the 6745- and 4767-keV transitions in ^{25}Mg, respectively, compared to the measured values of 0.18 and 0.41 mb. For the four high-energy transitions in ^{26}Mg in descending order of energy (see Table VI), the theoretically expected values of 14.8, 4.3, 1.7, and 0.77 mb agree roughly with the measured values of 4.55, 29.8, 2.29, and 0.68 mb, respectively, but the theory with these parameters gives considerably too low cross sections for the lower-energy transitions at 4967 and 4347 keV as well as for the three $M1$ transitions in ^{27}Mg. Lowering the giant-resonance energy by ~ 2 MeV does improve the agreement to some extent, but adjustment of this kind appears to be insufficient to explain the overall excess of $M1$ strength at the lowest γ-ray energies.

VI. SUMMARY

We have studied the energy levels of ^{25}Mg, ^{26}Mg, and ^{27}Mg via the (n,γ) reaction with thermal neutrons. Of the ~ 50 known [16] excited states in ^{25}Mg below the neutron separation energy, nine were found to be populated measurably in this reaction. The corresponding numbers are 55 out of ~ 144 states in ^{26}Mg and 10 out of ~ 37 in ^{27}Mg. For these states, we have determined accurate level energies and whenever possible good branching ratios. We have applied the direct-capture theory to reproduce (within a factor of ~ 2) the partial cross sections of the strong primary $E1$ transitions. However, a mechanism other than direct capture involving the giant magnetic resonance and possibly some other collective mode appears to be needed to explain the primary $M1$ transitions.

ACKNOWLEDGMENTS

Support for one of us (T.A.W.) was provided by the Oak Ridge Associated Universities and by the Research Corporation, and a sabbatical leave was provided by Edinboro University of Pennsylvania. We thank S. Kahane for his generous programming assistance and M. J. Martin and R. W. Sharpe for their helpful comments. This work was sponsored by the Department of Energy under Contracts No. DE-AC05-85OR21400 with Martin Marietta Energy Systems, Inc. (Oak Ridge) and No. W-7405-eng-36 with the University of California (Los Alamos).

[1] S. Raman, R. F. Carlton, J. C. Wells, E. T. Jurney, and J. E. Lynn, Phys. Rev. C **32**, 18 (1985).
[2] J. E. Lynn, S. Kahane, and S. Raman, Phys. Rev. C **35**, 26 (1987).
[3] S. Kahane, J. E. Lynn, and S. Raman, Phys. Rev. C **36**, 533 (1987).
[4] S. Raman, S. Kahane, R. M. Moon, J. A. Fernandez-Baca, J. L. Zarestky, J. E. Lynn, and J. W. Richardson, Phys. Rev. C **39**, 1297 (1989).
[5] S. Raman, J. A. Fernandez-Baca, R. M. Moon, and J. E. Lynn, Phys. Rev. C **44**, 518 (1991).
[6] J. E. Lynn, E. T. Jurney, and S. Raman, Phys. Rev. C **44**, 764 (1991).
[7] A. M. Lane and J. E. Lynn, Nucl. Phys. **17**, 563 (1960); **17**, 586 (1960); see also J. E. Lynn, *Theory of Neutron Resonance Reactions* (Clarendon, Oxford, 1968).
[8] A. H. Wapstra, Nucl. Instrum. Methods **292**, 671 (1990).
[9] S. Raman, in *Neutron Capture Gamma Ray Spectroscopy and Related Topics 1981*, edited by T. von Egidy, F. Gönnenwein, and B. Maier (Institute of Physics, Bristol, 1982), p. 357.
[10] S. F. Mughabghab, M. Divadeenam, and N. E. Holden, *Neutron Cross-Sections* (Academic, New York, 1981), Vol. 1, Part A, p. 1-1.

[11] P. Spilling, H. Gruppelaar, and A. M. F. op den Kamp, Nucl. Phys. **A102**, 209 (1967).
[12] P. Hungerford and H. H. Schmidt, Nucl. Instrum. Methods **192**, 609 (1982).
[13] W. V. Prestwich and T. J. Kennett, Can. J. Phys. **68**, 261 (1990).
[14] E. Selin and R. Hardell, Nucl. Phys. **A139**, 375 (1969).
[15] E. Selin and E. Wallander, Nucl. Phys. **A150**, 305 (1970).
[16] P. M. Endt, Nucl. Phys. **A521**, 1 (1990); P. M. Endt and C. van der Leun, *ibid.* **A310**, 1 (1978).
[17] F. Glatz, S. Norbert, E. Bitterwolf, A. Burkard, F. Heidinger, Th. Kern, R. Lehmann, H. Röpke, J. Siefert, and C. Schneider, Z. Phys. A **324**, 187 (1986).
[18] B. H. Wildenthal, Prog. Part. Nucl. Phys. **11**, 5 (1984).
[19] P. M. Endt, P. de Wit, and C. Alderliesten, Nucl. Phys. **A476**, 333 (1988); P. M. Endt, P. de Wit, C. Alderliesten, and B. H. Wildenthal, *ibid.* **A487**, 221 (1988).
[20] A. W. Kikstra, Z. Guo, C. van der Leun, P. M. Endt, S. Raman, T. A. Walkiewicz, J. W. Starner, E. T. Jurney, and I. S. Towner, Nucl. Phys. **A529**, 39 (1991).
[21] T. B. Ryves, J. Nucl. Energy **24**, 35 (1970).
[22] L. Koester, H. Rauch, and E. Seymann, At. Data Nucl. Data Tables **49**, 65 (1991).
[23] F. Meurders and G. de Korte, Nucl. Phys. **A249**, 205 (1974).
[24] G. P. A. Berg, R. Das, S. K. Datta, and P. A. Quin, Nucl. Phys. **A289**, 15 (1977).
[25] F. Meurders and A. van der Steld, Nucl. Phys. **A230**, 317 (1975).
[26] H. F. R. Arciszewski, E. A. Bakkum, C. P. M. van Engelen, P. M. Endt, and R. Kamermans, Nucl. Phys. **A430**, 234 (1984).
[27] M. Burlein, K. S. Dhuga, and H. T. Fortune, Phys. Rev. C **29**, 2013 (1984).
[28] A. G. W. Cameron, Can. J. Phys. **37**, 322 (1959). Cameron's semiempirical expression for $E1$ radiation widths is based on experimental data between $A \approx 30$ and $A \approx 240$ and has a weak A dependence. In the absence of sound experimental data, it is generally assumed that Cameron's expression can be extrapolated to lighter nuclei.
[29] A. Bohr and B. R. Mottelson, *Nuclear Structure* (Benjamin, Reading, 1975), Vol. II, p. 636.
[30] D. M. Brink, Ph.D. thesis, Oxford University, 1955 (unpublished).